UNIVERSITY OF CALIFORNIA, SAN DIEGO

Microcirculation Response to Ischemia-Reperfusion Injury

A thesis submitted in partial satisfaction of the requirements for the degree

Master of Science

in

Bioengineering

by

Marcelo Meirelles Leão de Barros

Committee in charge:

Professor Pedro Cabrales, Chair
Professor Geert Schmid-Schonbein
Professor John Watson

2014

The Thesis of Marcelo Meirelles Leão de Barros is approved, and it is acceptable in quality and form for publication on microfilm:

_____

_____

_____

Chair

University of California, San Diego

2014

For my parents and family for always unconditionally

supporting me and my dreams

Table of Contents

List of Figures

Abbreviations and Symbols

Abbreviations

NO – nitric oxide

NOS – nitric oxide synthase

eNOS – endothelial nitric oxide synthase

Np - nanoparticle

HR – heart rate

MAP – mean arterial pressure

RBC – red blood cell

WSR – wall shear rate

FCD – functional capillary density

GPx – glutathione peroxidase

GSH – glutathione

L-NAME – nitro-L-arginine methylester

LPO – lipid peroxidation

NOx – NO metabolites

ROS – reactive oxygen species

SOD – superoxide dismutase

Acknowledgements

I would like to thank the invaluable work of Cynthia Walser and Froilan Barra for the surgical preparations of the animals. Thanks must also be paid to Daniel Ortiz for his technical contributions and the continued support and exchange with all lab mates in the Cabrales Lab.

Vita

2012	Bachelor of Science, University of Texas, Austin
2014	Teaching Assistant, Department of Biomedical Engineering, University of California, San Diego
2014	Master of Science, University of California, San Diego

Publications

Resuscitation from hemorrhagic shock using polymerized hemoglobin compared to blood. Am J Emerg Med, 2014. 32(3): p. 248-55.

Abstract of the Thesis

Microcirculation Response to Ischemia-Reperfusion Injury

by

Marcelo Meirelles Leão de Barros

Master of Science in Bioengineering

University of California, San Diego, 2014

Professor Pedro Cabrales, Chair

In this study we show firstly the differences in physiologic response and tissue outcome on two distinct ischemic models, comparing hemodynamic, inflammatory, and histological parameters. The open window chamber model was utilized in Golden Syrian hamsters and tourniquet or compressive ischemic insult was applied to tissue for one hour, followed by reperfusion. Vasodilation, flow, leukocyte recruitment, wall shear rate, capillary perfusion and ultimate tissue outcome were assessed closely over the course of 24 hours post-ischemia. Despite the subtle differences in the hemodynamic response for both models, tissue cell death outcome for the tourniquet model was found to be significantly more pronounced. Secondly, a novel paramagnetic S-nitrosothiol nanoparticle was used with the compressive model in

order to validate the oxidative shielding properties of this proposed nanoparticle intervention. The treatment with this NO-releasing Np was shown to increase blood flow and reduce overall inflammatory response, thus demonstrating promise as a therapeutical avenue for ischemia and other inflammatory conditions.

I. Introductory Considerations

1.1 Ischemia – Reperfusion

Ischemia is a condition defined as constricted perfusion to an area of the body, followed by the restoration of the blood flow with the simultaneous recovery of oxygenation [1]. Several ischemic models have been developed, ranging from whole organ clamps to localized tourniquets [2-4].

The most fundamental consequence of ischemia is the absence of sufficient oxygen to maintain the metabolic demands of the cells. As a result, the cells initiate damage control and shift their resources and metabolism towards survival with an emphasis on anaerobic and metabolic pathway [1]. As free radicals start to increase within the cells, proteins, nuclei acids and the overall cell machinery becomes subject to damage.

The elucidation and understanding of ischemia and reperfusion injury are central to the physiological mechanisms of damage in pathological and trauma conditions such as myocardial infarction, stroke, vascular surgeries and interventions, organ transplantation, and vascular disease [1].

Years of research have revealed that further consequences of an ischemic insult include perfusion failure, characterized by the lowering of the functional capillary density [5], leukocyte recruitment and activation, formation of reactive compounds and the release of mediators (interleukins, platelet-activating factor, etc), leading eventually to loss of endothelial integrity and interstitial edema [6]. Prolonged periods aggravate the aforementioned phenomena by the activation and accumulation of white

blood cells that further results in more loss of perfusion and lack of oxygenation. This process is given the name of the reflow paradox whereby reperfusion and reflow actually cause augmented losses to the tissue by pathologically activating the immune system.

1.2 Open Window Chamber as an Ideal Model

The importance of the microcirculation to proper homeostasis and ultimate survival of an individual has been well established and understood. The microcirculation is, most of the time, the name given to the study of vessels below 100 microns. Such study carries within it the whole spectrum of research in a multitude of fields, ranging from understanding the immune system to drug transport and oxygenation of organs. The behavior of the microcirculation with therapeutic drugs, pathogens or an adverse or altered physiological state, is crucial for the prediction of patient or disease progression.

Microcirulatory intravital microscopy presents virtually limitless possibilities to the study of physiological questions in both health and disease states pertaining to these wide range of fields. The open window chamber model has been an established technique for the past 34 years, first described by Endrich and coworkers [4, 7]. It allows for superb and superior methods of analysis of the physiological response at the microcirulatory level, empowering the researcher with experimental validation *in vivo*.

This model permits one to ask questions ranging from angiogenesis in tumors [8], hemorrhagic shock and potential appropriate blood substitutes [9], hemodilution-anemia [10], sepsis shock[11], hypoxia [12], amongst others. It further makes it

reproducible to probe specific processes such as leukocyte adhesion and recruitment [13], tissue remodeling post biomaterial implantation [14], photoablation or coagulation studies [15], to mention a few.

Thus, this surgical model as an in-depth and wide encompassing tool towards the study of the microcirculation has been established and recognized.

1.3 Oxidative Stress

The cells, undergoing oxidative stress, will therefore attempt to generate oxidative shielding through a variety of mechanisms [1, 16]. This is a natural, expected defense response in which the cells attempt to protect themselves from a potential environmental hostility, effectively halting the spreading of possible infections.

Nevertheless, the increased oxidative stress is the primary pathogenic mechanism in endothelial dysfunction, resulting in limited NO bioavailability and ultimately microvascular inflammation [17].

The mitochondrion is the epicenter of where oxidative stress will truly occur, being therefore the most important organelle for cell fate in ischemia. The basic mechanism of action is that the mitochondria will start to divert electrons from its electron transfer pathway, and in the process generate reactive, radical species such as ROS or RNS.

It thus consists of a natural cellular biological response to stress albeit arguably an excessive or unnecessary one in different situations. Given these facts, it is a logical

step to attempt to diagnose and probe the mitochondria and to target it for pathology control [18].

Mitochondria oxidative stress can lead to apoptotic or necrotic cell fates [19]. These consist of terminal cellular states, with high levels of necrosis being generally undesirable.

1.3.1 SOD

Superoxide dismutase (SOD) is the first line of defense against oxidation, being ubiquitous in almost all cell types. This enzyme will catalyze the dismutation of oxygen superoxide into hydrogen peroxide plus oxygen. Superoxide is the most important reactive oxygen species and therefore SOD is an enzyme that provides essential antioxidant ability. Research has therefore been done utilizing SOD as a therapeutic target [20]. Targeted delivery of antioxidant enzymes to endothelial cells to prevent endothelial dysfunction was thus proposed as a reasonable avenue to avert pathological cascades. Previously, it has been tried to conjugate antibodies to endothelial surface marker molecule platelet endothelial cell adhesion molecule 1 (PECAM), targeting SOD in various organs [20]. SOD bound to anti-PECAM antibodies will enter endosomes in the endothelial lining, diminish the amount of superoxide anions and consequently inhibit cytokines from signaling pro-inflammatory cascades. Alternatively, other enzymes could have been utilized, such as catalase or angiotensin-II with differing effects.

1.3.2 eNOS

Endothelial Nitric Oxide Synthase usually poses very salutatory effects to the vasculature by oxidizing its substrate L-arginine to L-citrulline and NO·. However, the normal functioning of eNOS requires dimerization of the enzyme, presence of its substrate and the essential cofactor (6R)-5,6,7,8-tetrahydro-L-biopterin (BH4). In addition, it comprises the most important and prevalent NOS isoform in the vasculature, thus responsible for the majority of NO· production and vasodilation effects [21]. NO· has also the effect of inhibiting platelet and leukocytes activation and adhesion, being therefore simultaneously an anti-inflammatory and anti-thrombotic agent. It has been stated that endothelial NO· is the most important anti-atherogenic effector in the microcirculation, which poses the question of whether the nanoparticles here presented could be further used in treatment or suppression of atheroscleromas.

Reactive oxygen species generated during ischemia such as superoxide (O2-) reacts strongly with vascular NO· and forms peroxynitrite (ONOO-), which in turn causes the cofactor aforementioned to be oxidized by the peroxynitrite. The resulting lowered concentration of the cofactor promotes further reactive oxygen species to be produced in a process called eNOS uncoupling [21]. It is hence that an enzyme originally designed to correct oxidative imbalances and have protective vascular functions can become in fact prejudicial to the overall tissue microenvironment.

Lastly, of special attention is the mechanotransduction feature of eNOS that can be leveraged. This enzyme has been shown to become activated and induce the

generation of NO in cells that experience high shear forces and stretch [22]. Such quantitative parameter can be measured and at least in theory indicate higher levels of bioavailable NO. Although the signal transduction process of how eNOS is activated by shear forces has not been fully explained, there is growing literature and hypothesis being propounded in the recent decades [23]. In summary, the concept and model of cell tensegrity explain how integrins, the intermediate filaments and nuclear scaffolds provide an avenue for cellular mechanotransduction [24].

1.3.3 Glutathione

Thiols are able to serve as reducing agents, thus offering antioxidant properties to tissue. Cysteine's antioxidant effects are more commonly executed by glutathione (GSH), a crucial antioxidant in plants and animals, including microorganisms. Glutathione is essential to the well maintenance and functioning of the cellular environment due to its various biological functions. Briefly and most importantly, GSH is the (1) major endogenous antioxidant in cells, preventing cellular damage by reactive oxygen species, among other potentially damaging compounds; and (2) it further participates in the regulation of NO cycle [2]. Furthermore, it modulates cell death by apoptotic pathway signaling and represents the most fundamental redox buffer within mitochondria, which was previously stated as being the epicenter for oxidative damage [25]. Other important antioxidants include superoxidie dismutase, catalase and glutathione peroxidase.

1.4 Endothelial physiology

The most important and relevant component of the vasculature in ischemia-reperfusion studies are the endothelial cells, which line all blood vessels. These cells sense mechanical cues in the form of shear stress and modulate vascular tone through the production and excretion of vasodilators or vasoconstrictor compounds. The increased oxidative stress to the cells produces an endothelial dysfunction, decreasing NO bioavailability, inflammation, increased permeability and edema [1, 20]. Furthermore, the endothelium is able to sense the flow pattern and respond accordingly, where increased levels of ROS are generated for disturbed and irregular flow whereas regular flows produce decreased levels of ROS generation and higher NO bioavailability [26].

The endothelial is thus the component in the vasculature responsible for the local control of homeostasis, inflammatory mediators, hemostasis, permeability, cellular proliferation, as well as atherogenic factors [20, 26, 27].

1.5 Nitric Oxide

Different gases have been proposed to have therapeutic value to the amelioration of ischemia-reperfusion injury [1]. Nitric oxide has a vast array of biological functions, primarily being an antiginal molecule of fundamental physiological importance causing potent vasodilations. It further regulates the oxidative stress, having demonstrated to also possess anti-thrombotic and anti-inflammatory properties [16, 28].

Nitrite and nitrate anions are known end products of NO oxidation and therefore correlate well with endogenous NOS activity [29]. The roles of nitrite and nitrate are now slowly being further investigated, with promising new avenues for mitigating vascular diseases, especially in ischemia or hypoxia contexts [30]. Additionally, nitric oxide is scavenged by RBC as a function of hematocrit and oxygen tension in the vessels [31]. NO homeostasis is therefore of fundamental importance to the health of the microvasculature.

1.6 Innate Immune System

The activation of leukocytes and the mechanisms through which they will terminally stick to the endothelial has tremendous literature. Briefly, leukocyte activation can be prejudicial to the microcirculation outcome in two ways [32]. It has been proposed that due to large sizes of granulocytes and monocytes and stiff cytoplasm, a no-reflow phenomenon may ensue as they get increasingly trapped in the microcirculation. This would of course cause further hypoxia to the tissue as oxygen delivery becomes acutely impaired. Proteolytic activity has also been established as an undesirable consequence of leukocyte activation leading to further vascular permeabilization and edema [33].

1.7 Cell Fate

There are two main modes of cell death in ischemia, namely, apoptosis and necrosis. Necrosis is characterized for cell swelling leading to rupture and release of intracellular content. Necrosis has a strong immunostimulatory effect, further

aggravating inflammation and innate immune response. Conversely, apoptosis represents a deliberation on part of the cell to self-destruct, involving a series of complex signaling via caspases, especially caspase-3 [34].

It has thus far been generally accepted that apoptosis is a desirable pathway while necrosis is to be avoided at all costs. However, there is mounting evidence that apoptosis might actually cause increased damage through the release of ATP and other mediators [34].

Additionally, the role of autophagy in cell death during ischemia is also open for debate. Autophagy is characterized by the orchestrated self-degradation of the cellular organelles and components via lysosomes. There is evidence that autophagy in fact is an adaptive cellular response to a sublethal trauma or injury [35]. The well-known Hypoxic Inhibitory Factor, HIF, has been shown to be involved in autophagy regulation [36]. Furthermore, inducement of autophagy has been demonstrated to reduce ischemia-reperfusion injury and serve neuroprotective roles both *in vitro* and *in vivo* [35, 36]. Conversely, granulocyte colony stimulating factor, when systemically administered, has been shown to confer protective roles to cardiomyocytes via anti-autophagy mechanisms, independent of apoptosis [37]. It is of note that GCSF up regulated matrix metalloproteinases (MMP) and increased tissue macrophage presence, as opposed to its inhibition in the same study [37].

1.8 Significance

Ischemia and reduced blood flow in the microcirculation have wide reaching implications in various medical areas. Notably, a tourniquet ischemic insult is clinically analogous to stroke, in itself a major cause of death globally [38].

The research done in this study can potentially better elucidate the mechanisms of ischemia and reperfusion at the microcirculation level, which in turn could lead to better diagnosis, prevention and therapeutic interventions to disease states, with special emphasis of stroke damage, one of the leading causes of death in the US [38].

Furthermore, this study sets the foundation for the development of a different ischemic model that, although possessing similarities to the traditional tourniquet, presents etiological differences.

Of special scientific enquire is whether localized ischemia consists of a truly microscopic phenomenon or a mesoscopic one, whereby the ischemic tissue is interconnected with the adjacent tissue to an extent. The length or spatial reach of this aforementioned extent is debatable and often simply disregarded.

The study here presented further has the possibility to shed light on the role of NO in ischemia/reperfusion, which has been highly debatable [16, 29].

Ultimately, this study also serves as validation for the effectiveness and prospective salutatory effects of the delivery method used in the mitigation of acute vascular conditions and inflammation. Further research and testing must be done in order to fully understand both the biochemical and physiological consequences of the interventions hereby presented.

1.9 Hypothesis

The underlying hypothesis of this study is that the most immediate injury to the tissue is a resultant of the lack of metabolites and nutrients, primarily oxygen, being delivered to the cells. Secondary to this injury, and purported as more critical to the overall tissue insult and subsequent death, are the i) oxidative stress mediated by increased ROS levels and ii) leukocyte-driven damages.

Relatively little is known over the differences between the two different ischemic models here studied and it is hypothesized that both will behave distinctly.

It is thus hypothesized that the nanoparticles will reduce and alleviate overall tissue death and leukocyte activation in the microcirculation, effectively shielding the tissue from oxidative insult and inflammatory damage in either model.

Secondly, it is hypothesized that due to the diminished overall pressure applied to the tissue in the compression ischemic damage model, the vessels are maintained intact, without visible bleeding, thus enabling for a more efficacious means of delivering the payload.

II. Comparison of two ischemic models

2.1 Introduction

Several ischemic models have been developed, ranging from whole organ clamps [2, 3], localized tourniquets [4] and compressive models [6]. Nevertheless, there is a limited understanding over the differences between the two models concerning the physiological response. More importantly perhaps is the question of where the onset of the pathological state lies. To better elucidate the difference in two distinct models, namely compressive and tourniquet based models, ischemia was administered for one hour and hemodynamic parameters were followed for the subsequent 24 hours during reperfusion.

2.2 Ischemic Apparatus

The ischemic apparatus used previously was prone to user errors due to the lack of controllability and reproducibility over the force being exerted onto the tissue to be studied. Additionally, the stress distribution of the force applied was ill distributed due to the use of the microscope slide, which possesses a low Young's modulus. Previous research using the open window chamber model has seen acute inflammatory responses, vessel breakage and hemolysis even when very little force is applied [5]. This arguably suggests that the distribution of the forces is not spread equally, causing artificially higher insults that would have not otherwise be observed.

Previously, a coverslip slide was glued to an O-ring made of rubber and subjected to stress itself by the turning of a screw. The slide however possesses a low

Young's modulus, allowing it to bend and consequently alter the stress distribution, making it unequal. As such, it is pragmatically incredibly hard to lower the screw exactly at the center of the slide, which would consist in the only case scenario where the force distribution would be equalized. This seemingly irrelevant detail and triviality could well be the cause of vessel breakage and further deterioration of the microcirculation in ischemic studies.

In many experimental animal chambers, one side of the chamber was visibly more affected than the other, suggesting the stress propagation across the window was not equalized (data not provided).

2.3 Significance of Both Models

The models here studied have similarities but address different clinical complications. Compressive ischemic injury is an especially accurate model for the study of ulcerations in comatose patients lying in beds for long periods of time or that of diabetic patients that lose proprioception. The pathological mechanisms for both cases are not the same but the purported cause of injury is. Recurrent ischemia and reperfusion injury has been attributed to foot ulcers and bedsores in previous studies [39].

In diabetic patients, inducement of an ischemic environment, particularly in the soles of the feet, is triggered due to lack of proprioception sensitivity to the area. An aggravating factor arises from a high glucose environment and subsequent oxidative damage to the cells as previously reported in the literature [40]. The hyperglycemia

overwhelms the capacity for the cell to protect itself from oxidation, leading to abnormal cell death and damage [41].

As it can be seen, the studies of oxidative stress in ischemia/reperfusion studies have far reaching clinical potentials beyond the commonly established vascular diseases and pathologies.

2.4 Methods

2.4.1 Animal Models and Preparation

Male Syrian Golden hamsters weighting between 55 and 70 grams (Charles River Laboratories, Boston, MA) were fitted with a skinfold window chamber in their dorsal region. Animal handling and care followed the National Institutes of Health's Guide for the Care and Use of Laboratory Animals with all procedures being approved by the local animal care and use committee - IACUC. The window chamber preparation presents an intact microvascular network for both acute and chronic studies without anesthesia [4, 7, 42]. Briefly, the animals were prepared for chamber implantation under anesthesia. The window chamber consists of two titanium frames with a 15-mm diameter circular observation window. Sutures are used to lift the dorsal skin away from the animal and one frame of the titanium chamber is positioned in contact with the animal skin. One side of the skinfold is removed following the outline of the window until only a thin monolayer of retractor muscle and subcutaneous skin of the opposing side remain. Then, a cover glass is placed on the exposed tissue and held in place by the other frame of the chamber under a drop of saline. The animals were then allowed 2 days for recovery. Subsequently, they are anesthetized again and

arterial (carotid) and venous (jugular) catheters are implanted. The catheters are tunneled under the skin and exteriorized at the ventral side of the neck where they are attached to the chamber frame for ease of access. The animals were then allowed another day for recovery before the experiments were performed.

2.4.2 Microvascular Experimental Protocol

After the animals recovered from all the surgical procedures, they were not anesthetized again. The animal in the unanesthesized state was placed in a restraining tube with a longitudinal slit from which the window chamber protruded, then fixed to the microscopic stage of a transillumination intravital microscope (BX51WI, Olympus, New Hyde Park, NY). The animals were then given 20 min to adjust to the change in the tube environment before measurements were performed. Measurements were done using a 40X (LUMPFL-WIR, numerical aperture of 0.8, Olympus) water immersion objective.

After baseline measurements were taken, ischemia was applied to the chamber for 60 min. To the tourniquet model group, a tourniquet form of damage was applied, comprised of a rubber O-ring glued to a microscope slide and mounted into the 3D printed foundation; to the second group compression damage was applied, comprised of an air bubble glued to a microscope slide and the 3D printed foundation was mounted.

2.4.3 Systemic Parameters

Arterial pressure was extracted by connecting the arterial line catheter of the animal directly into a capacitive pressure transducer, which in turn feeds the signal to

a Biopac System, (MP 150, Biopac System, Inc., Santa Barbara, CA). MAP and heart rate can thus be easily measured based off the input signal. These parameters are not reported in this study, serving only as inclusion criteria for the decision to include the animals in the study.

Hematocrit levels (Hct) were determined from centrifuged arterial blood samples taken in heparinized capillary tubes (50 microliters). Plasma samples were then collected after centrifugation and freeze dried immediately.

The Hb content in blood was determined spectrophotometrically from a single drop of blood (HemoCue201®, Ängelholm, Sweden).

2.4.4 Inclusion Criteria

Healthy animals above 55 grams with no signs of distress, infection or complications were utilized in the experiments. Furthermore, if animals did not undergo any surgical bleeding and systemic parameters were within the normal range, they were deemed suitable for the experiments. Normal range was taken as follows: 1) MAP > 80 mmHg; 2) HR > 320 bpm; 3) systemic hematocrit (Hct) > 45%; 4) Hb count > 11 g/dL.

2.4.5 Ischemic Apparatus

To the backside of the chamber it was applied either a tourniquet or an air bubble compression to induce ischemia. The foundation and cup holder for control of the force applied were developed in SolidWorks and 3D printed, as shown in ***Figure A.1***. The tourniquet was composed of an O-ring shaped rubber and glued to a circular, thin microscope slide. Compression damage was achieved by gluing a single bubble

wrap instead. For the compression experiments, a different bubble apparatus was crafted before each experiment due to possible loss of air within the bubble and consequently physical integrity. The apparatus here presented was designed in order to provide superior reproducibility and control to the experimenter.

2.4.6 Functional Capillary Density (FCD)

FCD was evaluated by counting the amount of capillaries perfused by at least one RBC in the course of a 30-45 second visual inspection period. Ten distinct microscopic fields of view were utilized and followed throughout the course of the experiment for comparison. The relative change in FCD from baseline levels at the different time points is indicative of the extent of capillary perfusion to the tissue [5].

2.4.7 Microhemodynamic parameters

Velocity was computed by recording videos at a 1000 frames per second for a duration of 200 milliseconds and posteriorly performing a cross-correlation analysis. Briefly, each frame was broken down dynamically in regions of interest of sizes of 10 by 40 pixels (width by height) and the mathematical cross-correlation operation was performed against the regions of interest lying in the same vertical columns. The algorithm utilized corresponds to a mathematical cross-correlation method, as previously described [43]. A simple filter noise reduction was then used against the raw data and the resulting velocity values averaged and calibrated.

Blood flow was computed using the equation Q = pi * Vm * (D/2) ˆ 2 where Vm is the overall averaged velocity for that particular blood vessel. This previous

calculation assumes a parabolic velocity profile and has been found to be accurate for vessels of diameters ranging from 15-80 um and Hct in the range of 6-60% [43].

Wall shear rates were computed as follows. The raw data was analyzed in order to find the edges of the vessel, and then two boxes of pixels of size 20 were taken to calculate the wall shear rate. Wall shear rate is given as the slope of the velocity in the radial direction. The raw values were subsequently applied cutoffs of mean ± SD and multiplied by the frame rate, yielding the correct units of 1/seconds.

The same vessels were followed throughout the entirety of the experiment for direct comparison against baseline and increased statistical robustness.

2.4.9 Leukocyte Count

Leukocytes were counted for a 30 seconds window by visual inspection posterior to infusion of the organic fluorescent dye Rhodamine 6G [44]. Rolling leukocytes were defined as those moving slower than the blood flow whereas sticking or adhering leukocytes were counted if immobile for the duration of the observation window. An imaginary axis perpendicular to the vessel in the radial direction was utilized for the counting of rolling leukocytes. Sticking leukocytes were counted if within the field of view.

2.4.10 Tissue Viability

The occurrence of apoptosis was assessed with the terminal transferase mediated dUTP nick end-labelling (TUNEL) assay (In Situ Cell Death Detection Kit, TMR fluorescein, Roche Diagnostics, Alameda, CA). The kits offer a direct TUNEL detection method for maximum sensitivity and minimal background. All steps were

performed according to the supplier instructions. Briefly, the hamsters were euthanized immediately after intravital microscopic imaging and the window tissue was harvested and fixed. Sections were permeabilized with 0.1M citrate buffer, then microwaved and cooled rapidly. The sections were then incubated with terminal deoxynucleotidyl transferase (TdT) enzyme for 1h at 37 °C in the dark. The reactions were terminated by rinsing three times in phosphate buffered saline, and the tissue was protected with a coverslip. Sections of green-labeled cells (excitation wavelength: 450B500 nm and detection: 515B565 nm) were examined without delay with a fluorescence microscope.

2.4.11 Data Analysis

Results were presented as means ± standard deviation (SD). Data between groups were analyzed utilizing Two-Way ANOVA tests, with posterior multiple Bonferroni tests evaluated when appropriate. For some parameters, Kruskal Wallis T-student tests were used so as not to have loss of data in the cases where certain time points prevented ANOVA evaluations. Microhemodynamic measurements were compared against baseline levels obtained prior to experimentation. Data are presented as absolute values or as ratios relative to baseline. A ratio of 1.0 translates into no alteration from baseline, whereas lower or higher ratios are indicative of proportional changes from baseline levels (i. e. 1.5 would mean a 50% increase). The same vessels and functional capillary fields were followed so that direct comparisons with their baseline levels could be performed, yielding more robust statistics for small sample populations. All statistical calculations were performed using GraphPad Prism 4.01

(GraphPad Software, Inc., San Diego, CA) with statistical significance attributed to values of $P < 0.05$.

2.5 Results

2.5.1 Systemic Parameters

All systemic values, including hemoglobin count, mean arterial pressure, heart rate and blood gases did not significantly alter throughout the entire protocol (data not shown). Furthermore, the values remained within the normal expected physiological range for Syrian hamsters, as previously reported [9].

2.5.2 FCD

Figure 2.1 depicts the changes in functional capillary density (FCD) for the duration of the experiment. FCD was significantly reduced for the tourniquet group to about 85% of its baseline levels and remained low for the first two hours of reperfusion, being restored at 24h post-ischemia. Furthermore, the tourniquet resulted in a statistically inferior perfusion post-ischemia as compared to the pressure model. FCD values at 2 hours during reperfusion were reported to be 0.81 ± 0.05 and 0.93 ± 0.05 for the tourniquet and compressive model, respectively. The compressive model did not present significant changes from baseline for the whole experimental design.

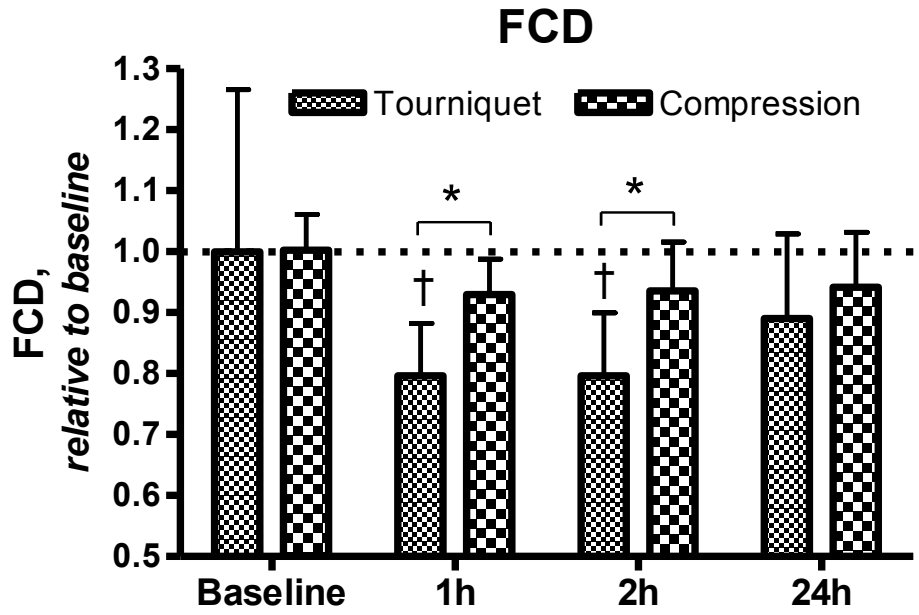

Figure 2.1. Functional Capillary Density for both ischemia models.
FCD normalized relative to baseline. Baseline values were quantified as 8.9 cm-2 (n = 10) where 'n' indicates the amount of animals included.

2.5.3 Microhemodynamics

The measured hemodynamics parameters are summarized in ***Figure 2.2***. The tourniquet group observed mild arterial vasoconstriction (10% of baseline) along with mild venular vasodilation (also 10%). The compressive model also demonstrated very mild arteriolar contraction (92% of baseline) at the two hours time point but showed no difference from baseline for the veins. The two groups were found to be statistically equivalent throughout the entire protocol for the diameter parameter. Blood flow was observed to be restricted post-ischemia for the two groups.

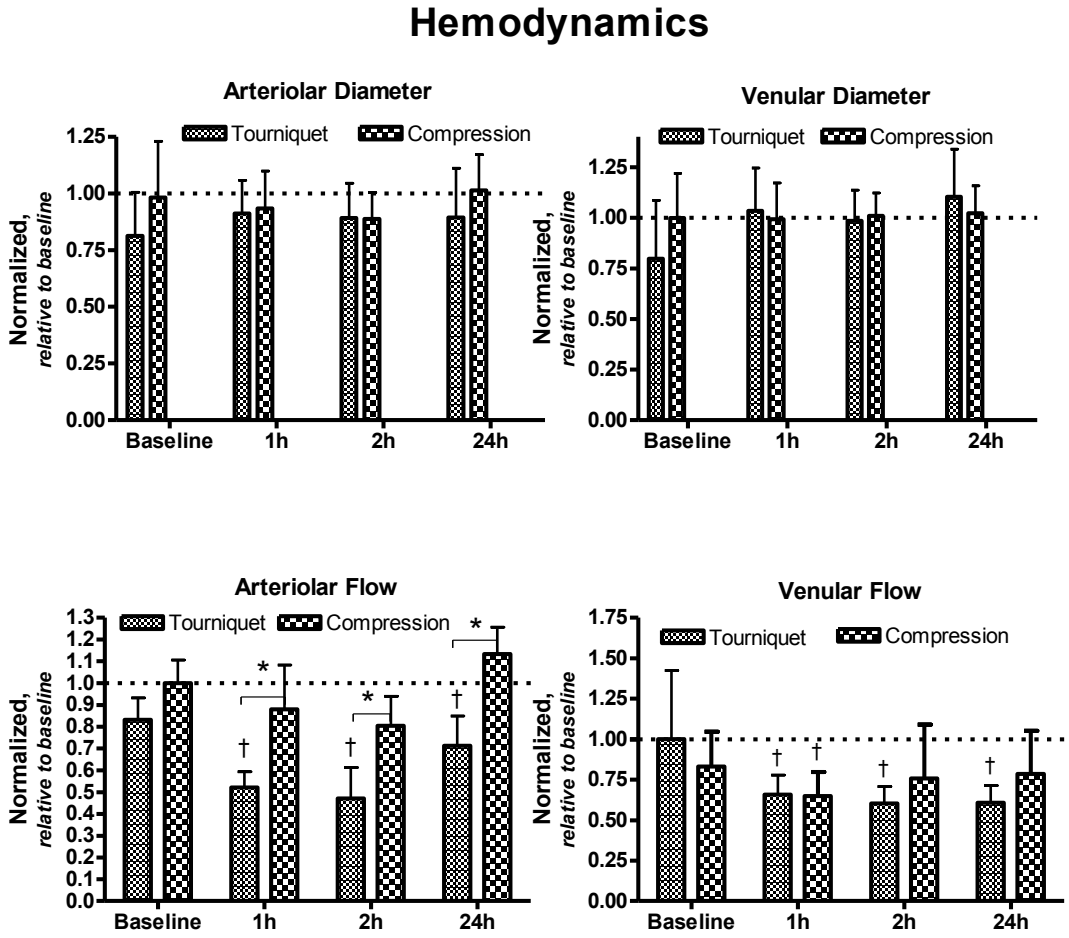

Figure 2.2. Microvascular hemodynamic data relative to baseline during reperfusion. Values are shown as changes relative to baseline where 1.0 = 100% of baseline. *P < 0.05 compared with baseline; †P < 0.05 compared between groups. Baseline diameters, (A) and (B), for each animal group were as follows: Tourniquet (arterioles : 63.9 ± 16.1, n = 24; venules [V]: 46.2 ± 9.3, n = 25; Compression (A: 48.1 ± 11.7, n = 20; V: 47.4 ± 10.3, n = 14); Calculated baseline blood flow, (C) and (D), (nL/s, mean ± SD) for each animal group were as follows: Tourniquet (arterioles [A]: 10.7 ± 8.7, n = 20; venules [V]: 3.9 ± 2.7, n = 20); Compression (A: 8.4 ± 5.7, n = 14; V: 6.4 ± 3.4, n = 9); with 'n' indicating number of vessels studied.

2.5.4 Wall Shear Rate

Wall shear rate is given by ***Fig*ure 2.3.** The arterioles and venules behaved differently for each group studied. For the tourniquet model, within the arterioles, the wall shear rate was maintained at basal values at one hour but increased by almost

50% two hours into reperfusion. The wall shear rate was found to have been restored 24h after ischemia.

The compressive model on the other hand had its wall shear rate parameter reduced to 75% of baseline at 1h and slowly restored at the 2h time point. At 24 hours, the computed wall shear rate was found to be statistically higher than baseline values. Thus, the tourniquet model experienced an overall increase in wall shear rates whereas the compressive ischemic model demonstrated a depression for the wall shear rate measurements. The shear rate for the tourniquet model at 2h post-ischemia was found to be statistically significant to the compression group.

Concerning the venules, both groups behaved similarly, with wall shear rate reductions to 89% and 78% for the tourniquet and compression, respectively, relative to baseline. Throughout the whole protocol, the venular shear rates were not significantly altered from these reduced values. The compression model never exhibited a normalization of its venular WSR.

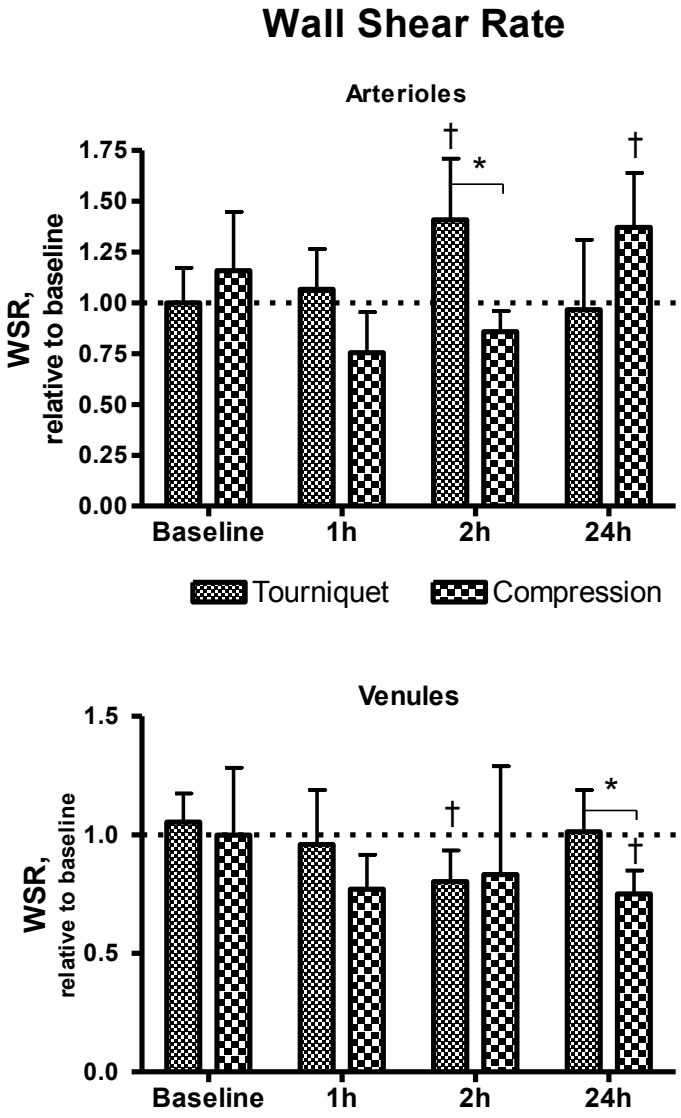

Figure 2.3. Wall shear rate data relative to baseline during reperfusion for both models. Values are shown as relative to baseline where 1.0 = 100% of baseline. Wall shear rate (1/s, mean ± SD) for each animal group were as follows: Tourniquet (arterioles [A]: 65.4 ± 10.6, n = 17; venules [V]: 54.3 ± 21.1, n = 18); Compression (A: 57.2 ± 37.9, n = 8; V: 35.7 ± 20.2, n = 6); with 'n' indicating number of vessels included.

2.5.5 Leukocyte Count

The graphs relating to rolling and immobilized leukocytes are presented in ***Figure.*** **2.4.** The data is presented as fractions from total count throughout the entire

protocol. Rolling leukocytes were found to increase for the first observed two hours post-ischemic injury and then normalize back to basal levels 24 hours later. Compressive ischemia elicited higher rolling leukocyte counts though the observed differences were not found to be statistically significant. The highest fractions occurred at the 2h time point for both groups.

Immobilized leukocytes, shown in panel B, were found to consistently increase for both models in the two hours following tissue insult. The fraction of measured immobilized leukocytes at baseline was close to 10% for both groups. This percentage was not restored during experimentation. One-hour post ischemia, sticking leukocyte fraction was computed to be close to 30% for both groups. At the two hours, statistical significance was reported, with tourniquet ischemia stimulating close to 60% of all observable sticking leukocytes as compared to 31% in the compressive group.

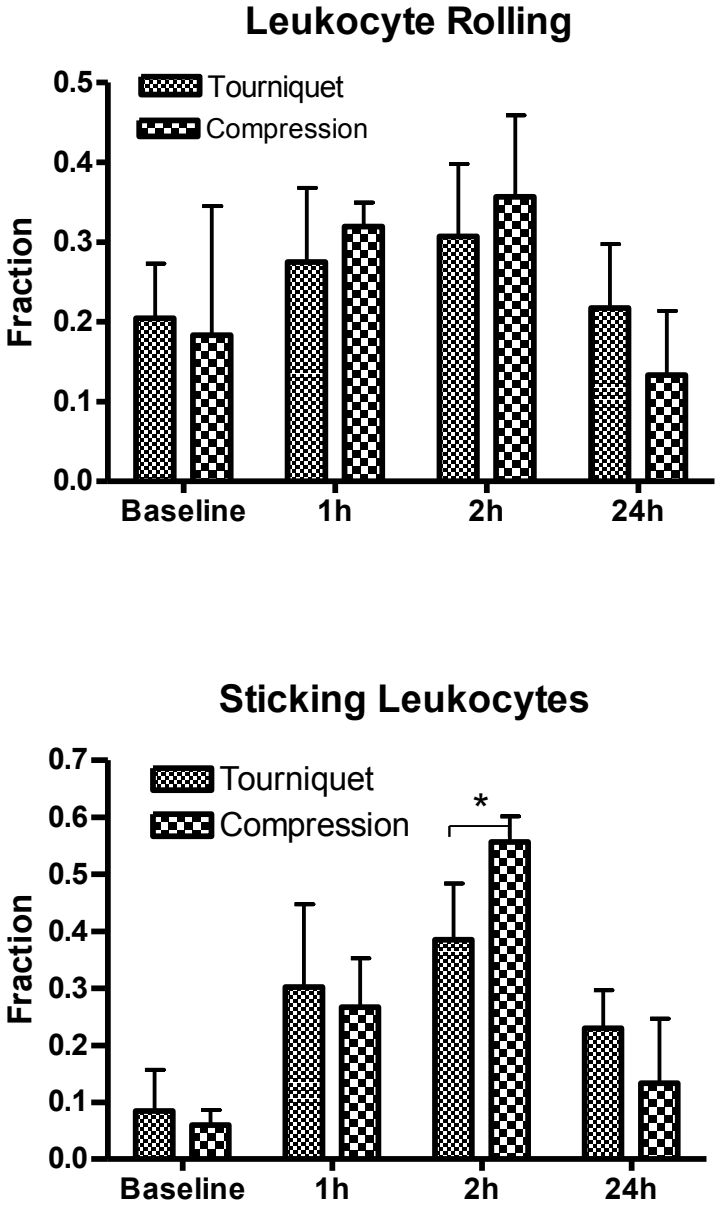

Figure 2.4. Leukocyte Count for both ischemic models.
Leukocyte data profile fraction. The values represent the fraction of leukocytes observed for that particular time point as compared to the total of leukocytes observed for all time points within the same individual. A value of 0.25 in the immobilized leukocyte graph represents that out of all the leukocytes counted as immobilized, one quarter of them were seen during that corresponding time point. Values are given as percentages ± SD. Panel (A) shows rolling leukocytes while panel (B) contains immobilized leukocyte count throughout the experiment.

2.5.6 Tissue Survivability

The histological cell fate data is summarized on ***Figure* 2.5**. All immunohistochemistry measurements were performed on fixed tissue collected at 24 hours post-ischemia. Panel (A) breaks down cell death into early/late apoptotic and necrotic cell fates whereas panel (B) shows the absolute summation of these two distinct cell fates. Under normal, baseline conditions, apoptosis and necrosis are observed at the same percentage and rate, namely near 8%.

The tourniquet model group showed a statistically higher percentage of cell death as compared to the compressive model, with over 60% of cells undergoing death pathways. The compressive model was found to have 30% total cell death, therefore about half of cellular death observed in the tourniquet model.

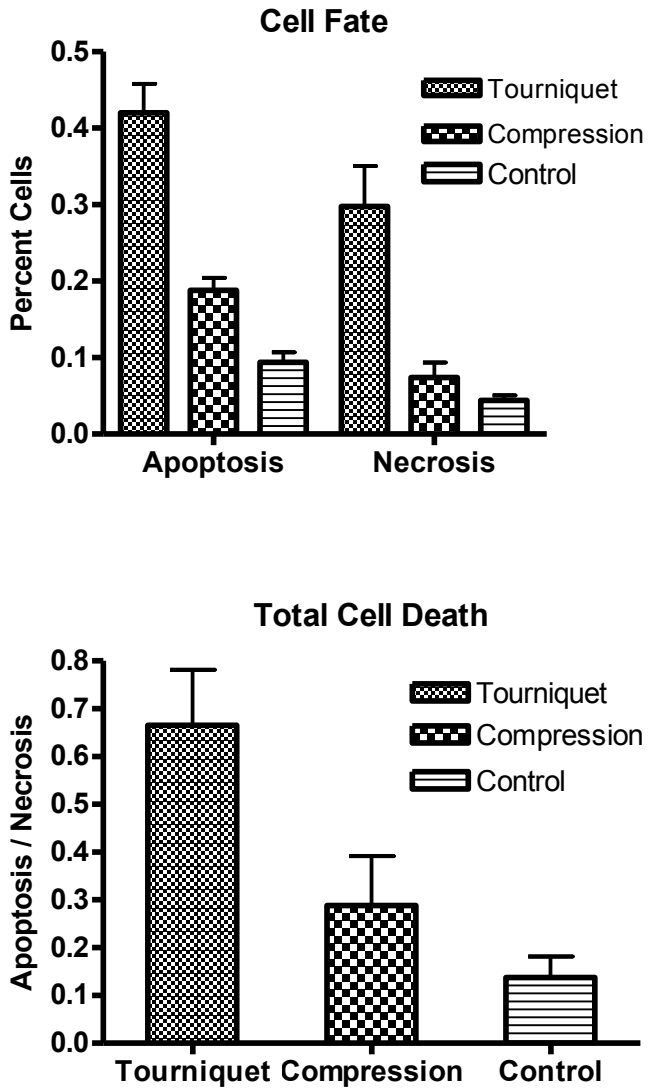

Figure 2.5. Histological data 24h post ischemia for both models.
Cell fate count via immunohistochemistry. Panel A divides the data into apoptotic and necrotic cell fates. Panel B reports the total summation of apoptotic and necrotic cells. All values are percent from total cell count in the fields of views. All groups were found to be statistically significant compared to one another.

2.6 Discussion

The principal finding of this study is that compression damage demonstrated superior recovery from IR injury despite the mildness of the ischemia insult itself and

the higher degree of inflammatory response as inferred from the leukocyte count. Moreover, the two different modes of ischemia behaved in consistently distinct manners even though this difference was not a drastic one.

An inflammatory response can take up to 48 hours, but given the small insult that is being generated in this protocol, it is expected that by 24 hours, the microcirculatory parameters would be restored to normality. Concerning the sterile inflammatory response, the rolling leukocyte profile for both models was found to be similarly flat. This initially seems to suggest that both models are recruiting leukocytes to the affected area equally or at the same rate. However, the data, as it is presented and computed, does not account for the flow within the vessels. In the compressive model, blood flow is reduced as compared against the tourniquet, and therefore it is expected that the flux of leukocytes would be lower. Conversely, the higher flux in the vessels of the animals that underwent tourniquet injury reveals a more numerous leukocyte count. Hence, the change in blood flow effectively masks the results.

The aforementioned data is corroborated by the fact that there is a clear difference in immobilized leukocyte profile in the two cases. More recruitment translates into more activation and ultimately extravasation of white blood cells. This suggests a greater degree of damage and by inference, oxidative and metabolic damages. Coupled to the inflammatory response are the reduced velocities and blood flow within the vessels, in particular within the venules. The lowered velocity facilitates leukocytes to bind and to interact with the endothelial lining. Additionally, adhesion-inducing molecules could be enhancing the leukocyte endothelial interaction.

In any case, leukocyte count as it was described in this study was not sufficient to predict tissue outcome. This could also suggest that the presence of the leukocytes in the compressive model yielded a salutatory effect to the tissue and its overall survivability. There is therefore a range of inflammatory response that is beneficial to the cells affected by ischemia but beyond such range, the presence of leukocytes could prove harmful.

The clear difference in cell death is presumably due to the overall reduced and more prolonged perfusion in the tourniquet model that ensues after ischemia. Additionally, the observed hemolysis in tourniquet models (not shown) causes Hb to become acellularized, which in turn generates further ROS due to Hb auto-oxidation [45]. Thus, the reperfusion injury caused by the tourniquet model is significantly higher than that of the compression model.

2.7 Future Work

A more in depth analysis of the underlying biochemistry ought to be done for the two models. It is likely that the hemolysis and vessel breakage seen in the tourniquet model initiates further inflammatory cascades not otherwise seen in the compressive model.

One hour of ischemia utilizing the compressive model is arguably an ideal model to study the damage caused by the lack of oxygen while maintaining reperfusion injury to a minimum. One could then evaluate and analyze more in-depth the biochemistry and metabolic state of the tissue post-ischemia without the

confounding effects of reperfusion injury, which is triggered by leukocyte recruitment, activation and oxidative damage.

III. Effects on Microcirculation Secondary to Ischemia Using a Novel S-nitrosothiol Nanoparticle Intervention

3.1 Introduction

There has been growing attention in developing NO based interventions due to its established biological relevance and role. A rational therapeutic goal is to therefore balance the NO bioavailability, disrupted due to ischemia. A delicate balance between the scavenging and production of NO exists and ought to be preserved [31, 46]. In light of this model, S-nitrosothiols (RSNO) therapeutic compounds have been given attention as potential vehicles for bioactive nitrogen and NO delivery, having seen some margin of success [47].

Current strategies to mitigate damage through the tinkering of the metabolic demands and needs of the cells will be here briefly explored. As previously expounded on the importance of eNOS for NO synthesis and overall tissue outcome, being able to increase eNOS activity should be a sound rationale for disease therapy. L-arginine, the precursor for eNOS, has been successfully demonstrated to significantly reduce tissue damage, with increased perfusion in the lungs after hemorrhagic shock [48].

Currently, there is a need for the alleviation of tissue damage to areas of surgical procedure or organs downstream of surgical clamps. The development of a drug vehicle that could target and localize within a desired tissue could prove remarkably advantageous.

The importance of the bioavailability of NO having been established, several drugs that attempt to modulate NO in the vasculature for the purposes of preventing

cardiovascular dysfunction have been studied [49]. These drugs however suffer from a myriad of downfalls ranging from potential toxicity, lack of specificity or basic mechanistic understanding of action, along with high costs.

3.2 Nanoparticles as Superior Localized Drug Delivery Vehicles

There is a growing need for vascular drug delivery vehicles such as nanoparticles that are safe and efficacious towards treatment of vascular inflammatory conditions. Special attention must be given to ischemia-reperfusion insults, sepsis and stroke scenarios [50]. The rationale for developing these nanoparticles as therapeutic vehicles of biopharmaceuticals is threefold.

Firstly the often necessity of localization of the drug to the affected areas and the biological inherent compartmental barriers the drug must face demands precision in their localization. Ultimately, the risk to benefit analysis must favor the beneficial side by optimizing localization and timing of the drug, therefore increasing overall efficacy and drug action [51].

Secondly, the paramagnetic physical property of the nanoparticles used in this study confers them the advantage to even further localize drug delivery and potentially mitigate or even abolish systemic toxicity effects [52].

Thirdly, it concerns to the pharmokinetics of the intervention. Nanoparticles commonly have the downfall of being eliminated quickly by renal filtration and leukocyte phagocytosis [53]. By concentrating the payload onto a small area, a much longer and sustained effect can be achieved [47].

Given the current knowledge over the biochemistry of cellular damage and the triggers toward necrosis and apoptosis, a logical strategy to remediate or alleviate cellular damage is to target the mitochondria [54]. This strategy is precisely what is being attempted with the proposed intervention.

3.3 Model of choice

The compressive ischemic model was chosen for two reasons: (1) it more closely resembles the pathogenesis of conditions associated with skin and muscle, e.g. ulcerations and bedsores [39, 55] and (2) because it presents less associated aggravating factors such as redness along vessel breakage. This seemingly trivial pragmatic reason allows for better elucidation over the biochemical causes and mechanisms of pathology, taking away some confounding factors such as the ones aforementioned.

3.4 Methods

3.4.1 Animal Models and Preparation

Male Syrian Golden hamsters weighting between 55 and 70 grams (Charles River Laboratories, Boston, MA) were fitted with a skinfold window chamber in their dorsal region. Animal handling and care followed the National Institutes of Health's Guide for the Care and Use of Laboratory Animals with all procedures being approved by the local animal care and use committee - IACUC. The window chamber preparation presents an intact microvascular network for both acute and chronic studies without anesthesia [4, 7, 42]. Briefly, the animals were prepared for chamber

implantation under anesthesia. The window chamber consists of two titanium frames with a 15-mm diameter circular observation window. Sutures are used to lift the dorsal skin away from the animal and one frame of the titanium chamber is positioned in contact with the animal skin. One side of the skinfold is removed following the outline of the window until only a thin monolayer of retractor muscle and subcutaneous skin of the opposing side remain. Then, a cover glass is placed on the exposed tissue and held in place by the other frame of the chamber under a drop of saline. The animals were then allowed 2 days for recovery. Subsequently, they are anesthetized again and arterial (carotid) and venous (jugular) catheters are implanted. The catheters are tunneled under the skin and exteriorized at the ventral side of the neck where they are attached to the chamber frame for ease of access. The animals were then allowed another day for recovery before the experiments were performed.

3.4.2 Microvascular Experimental Setup

After the animals recovered from all the surgical procedures, they were not anesthetized again. The animal in the unanesthesized state was placed in a restraining tube with a longitudinal slit from which the window chamber protruded, then fixed to the microscopic stage of a transillumination intravital microscope (BX51WI, Olympus, New Hyde Park, NY). The animals were then given 20 min to adjust to the change in the tube environment before measurements were performed. Measurements were done using a 40X (LUMPFL-WIR, numerical aperture of 0.8, Olympus) water immersion objective.

After baseline measurements were taken, ischemia was applied to the chamber for 60 min. To the tourniquet model group, a tourniquet form of damage was applied, comprised of a rubber O-ring glued to a microscope slide and mounted into the 3D printed foundation; to the second group compression damage was applied, comprised of an air bubble glued to a microscope slide and the 3D printed foundation was mounted.

3.4.3 Systemic Parameters

Arterial pressure was extracted by connecting the arterial line catheter of the animal directly into a capacitive pressure transducer, which in turn feeds the signal to a Biopac System, (MP 150, Biopac System, Inc., Santa Barbara, CA). MAP and heart rate can thus be easily measured based off the input signal. These parameters are not reported in this study, serving only as inclusion criteria for the decision to include the animals in the study.

Hematocrit levels (Hct) were determined from centrifuged arterial blood samples taken in heparinized capillary tubes (50 microliters). Plasma samples were then collected after centrifugation and freeze dried immediately.

The Hb content in blood was determined spectrophotometrically from a single drop of blood (HemoCue201®, Ängelholm, Sweden).

3.4.4 Inclusion Criteria

Healthy animals above 55 grams with no signs of distress, infection or complications were utilized in the experiments. Furthermore, if animals did not undergo any surgical bleeding and systemic parameters were within the normal range,

they were deemed suitable for the experiments. Normal range was taken as follows: 1) MAP > 80 mmHg; 2) HR > 320 bpm; 3) systemic hematocrit (Hct) > 45%; 4) Hb count > 11 g/dL.

3.4.5 Ischemic Apparatus

A tourniquet or an air bubble compression to was applied to the backside of the chamber to induce ischemia. The foundation and cup holder for control of the force applied were developed in SolidWorks and 3D printed, as shown in ***Figure A.1***.

The tourniquet was composed of an O-ring shaped rubber and glued to a circular, thin microscope slide. Compression damage was achieved by gluing a single bubble wrap instead. For the compression experiments, a different bubble apparatus was crafted before each experiment due to possible loss of air within the bubble and consequently physical integrity. The apparatus here presented was designed in order to provide superior reproducibility and control to the experimenter.

3.4.6 Functional Capillary Density (FCD)

FCD was evaluated by counting the amount of capillaries perfused by at least one RBC in the course of a 30-45 second visual inspection period. Ten distinct microscopic fields of view were utilized and followed throughout the course of the experiment for comparison. The relative change in FCD from baseline levels at the different time points is indicative of the extent of capillary perfusion to the tissue [5].

3.4.7 Microhemodynamic Parameters

Velocity was computed by recording videos at a rate of 1000 frames per second for a duration of 200 milliseconds and posteriorly performing a cross-

correlation analysis. Briefly, each frame was broken down dynamically in regions of interest of sizes of 10 by 40 pixels (width by height) and the mathematical cross-correlation operation was performed against the regions of interest lying in the same vertical columns. The algorithm utilized corresponds to a mathematical cross-correlation method, as previously described [43]. A simple filter noise reduction was then used against the raw data and the resulting velocity values averaged and calibrated. Blood flow was computed using the following equation: Q=pi*Vm*(D/2)^2 where Vm is the overall averaged velocity for that particular blood vessel. This previous calculation assumes a parabolic velocity profile and has been found to be accurate for vessels of diameters ranging from 15-80 um and Hct in the range of 6-60% [43].

Wall shear rates were computed as follows. The raw data was analyzed in order to find the edges of the vessel, and then two boxes of pixels of size 20 were taken to calculate the wall shear rate. Wall shear rate is given as the slope of the velocity in the radial direction. The raw values were subsequently applied cutoffs of mean ± SD and multiplied by the frame rate, yielding the corrected units of 1/seconds.

The same vessels were followed throughout the entirety of the experiment for direct comparison against baseline and increased statistical robustness.

3.4.8 Nanoparticles preparation

The nanoparticles used in this study are a derivative of already described and characterized nanoparticles [47]. The particles were stored in the fridge up until 30 minutes prior to infusion, from which point a dosage of 20mg/Kg was collected and

subsequently solubilized in 0.1 mL of heparinized saline and sonicated for 5 min. The solution was then centrifuged for 2 min at 3300 rpm and posteriorly re-sonicated and re-centrifuged for another round. Finally, the supernatant was collected and infused immediately after cessation of ischemia. The preparation here presented was developed in-house after a series of optimizations envisioning improved solubility of the nanoparticles.

3.4.9 Leukocyte Count

Leukocytes were counted for a 30 seconds window by visual inspection posterior to infusion of the organic fluorescent dye Rhodamine 6G [44]. Rolling leukocytes were defined as those moving slower than the blood flow whereas sticking or adhering leukocytes were counted if immobile for the duration of the observation window. An imaginary axis perpendicular to the vessel in the radial direction was utilized for the counting of rolling leukocytes. Sticking leukocytes were counted if within the field of view.

3.4.10 Tissue Viability

The occurrence of apoptosis was assessed with the terminal transferase mediated dUTP nick end-labelling (TUNEL) assay (In Situ Cell Death Detection Kit, TMR fluorescein, Roche Diagnostics, Alameda, CA). The kits offer a direct TUNEL detection method for maximum sensitivity and minimal background. All steps were performed according to the supplier instructions. Briefly, the hamsters were euthanized immediately after intravital microscopic imaging and the window tissue was harvested and fixed. Sections were permeabilized with 0.1M citrate buffer, then

microwaved and cooled rapidly. The sections were then incubated with terminal deoxynucleotidyl transferase (TdT) enzyme for 1h at 37 °C in the dark. The reactions were terminated by rinsing three times in phosphate buffered saline, and the tissue was protected with a coverslip. Sections of green-labeled cells (excitation wavelength: 450B500 nm and detection: 515B565 nm) were examined without delay with a fluorescence microscope.

3.4.11 Data Analysis

Results were presented as means ± standard deviation (SD). Data between groups were analyzed utilizing Two-Way ANOVA tests, with posterior multiple Bonferroni tests evaluated when appropriate. For some parameters, Kruskal Wallis T-student tests were used so as not to have loss of data in the cases where certain time points prevented ANOVA evaluations. Microhemodynamic measurements were compared against baseline levels obtained prior to experimentation. Data are presented as absolute values or as ratios relative to baseline. A ratio of 1.0 translates into no alteration from baseline, whereas lower or higher ratios are indicative of proportional changes from baseline levels (i. e. 1.5 would mean a 50% increase). The same vessels and functional capillary fields were followed so that direct comparisons with their baseline levels could be performed, yielding more robust statistics for small sample populations. All statistical calculations were performed using GraphPad Prism 4.01 (GraphPad Software, Inc., San Diego, CA) with statistical significance attributed to values of $P < 0.05$.

3.5 Results

3.5.1 Systemic Parameters

All systemic values, including hemoglobin count, mean arterial pressure, heart rate and blood gases did not significantly alter throughout the entire protocol (data not shown). Furthermore, the values remained within the normal expected physiological range for Syrian hamsters, as previously reported [9].

3.5.2 FCD

Functional capillary density changes are presented in ***Figure 3.1***. The two groups were statistically equivalent for the entirety of the experiment, with no significance attributed. Perfusion was found to be mildly reduced to 93% of baseline levels for both models at the 1h time point. FCD was not statistically distinct from baseline at any point during the protocol for either group.

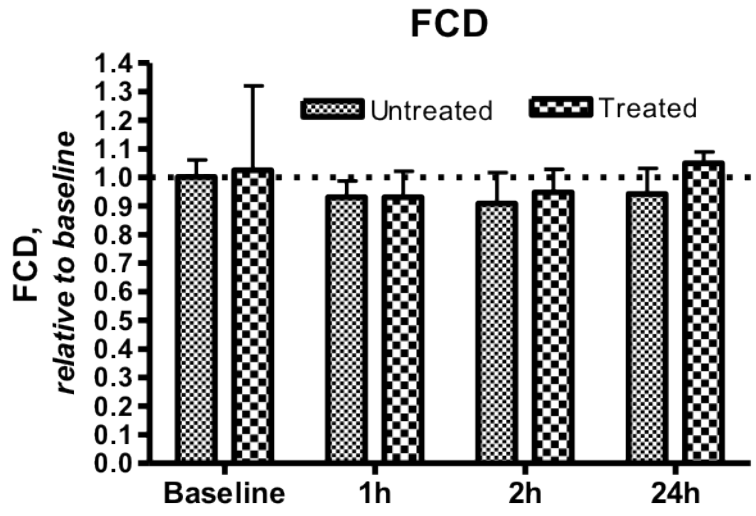

Figure 3.1. Functional capillary density for untreated and Np-treated groups.
Functional Capillary Density FCD normalized relative to baseline. Baseline values were 8.2 cm-2 (n = 9) where 'n' represents the number of animals included.

3.5.3 Microhemodynamics

The measured hemodynamics parameters are summarized in ***Figure 3.2***. No discernible vasoconstriction or vasodilation was observed for either group in the arteries or venules. As such, the arteriolar and venular diameters remained constant for the duration of the experiment. Blood flow measurements are depicted in panels (C) and (D), where vascular flow was found to increase in the compression model for the observed two hours of reperfusion. Arteriolar blood flow was reported to be significantly higher for the compression model, seeing increases in up to 30%. Venular flow was also calculated to be greater though not statistically significant.

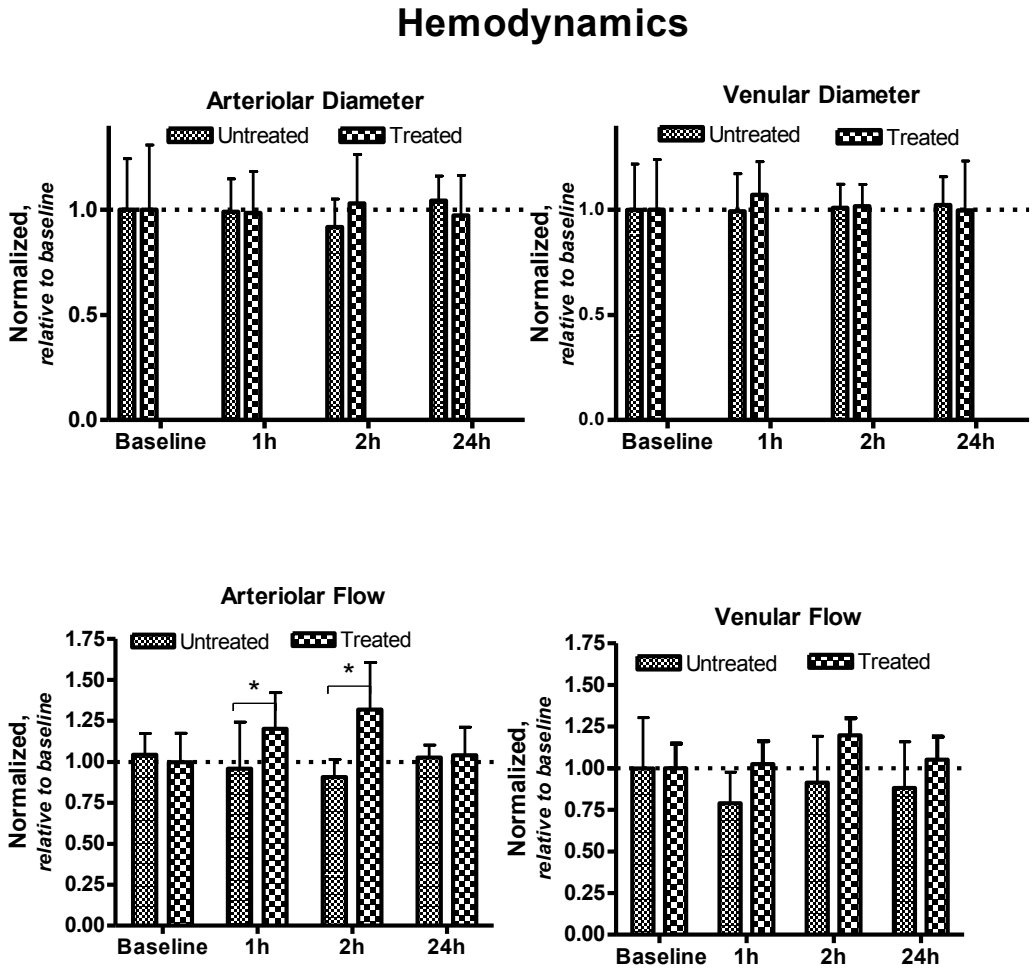

Figure 3.2. Microvascular hemodynamic relative to baseline for untreated and Np-treated groups. Values are shown as changes relative to baseline where 1.0 = 100% of baseline. *P < 0.05 for comparisons between groups. Baseline diameters, (A) and (B), for each animal group were as follows: Untreated (arterioles [A]: 48.0 ± 10.0, n = 15; venules [V]: 47.2 ± 10.0, n = 10; Np-Treated [A]: 51.8 ± 13.9, n = 15; [V]: 44.5 ± 10.7, n = 17); Calculated baseline blood flow, (C) and (D), (nL/s, mean ± SD) for each animal group were as follows: Untreated [A]: 10.7 ± 8.7, n = 11; [V]: 3.9 ± 2.7, n = 9); Np-treated [A]: 8.4 ± 5.7, n = 14; [V]: 6.4 ± 3.4, n = 16); with 'n' indicating number of vessels studied.

3.5.4 Wall Shear Rate

Wall shear rate parameter (units of inverse seconds) is given by ***Figure 3.3***. The wall shear rates behaved in accordance to the blood flow parameter. Therefore, arteriolar blood flow for the treated animals was found to be statistically greater to about 150% from baseline levels for the two hours of reperfusion studied. At 24h,

arteriolar WSR was still greater than the untreated group and not yet normalized to baseline levels. Venular shear rates dropped to about 80% relative to baseline at the first hour and normalized for the treated group at the 2h time point. The untreated group on the other hand remained with venular shear rates at significantly lower values even 24 hours post ischemia, therefore not normalizing the shear forces.

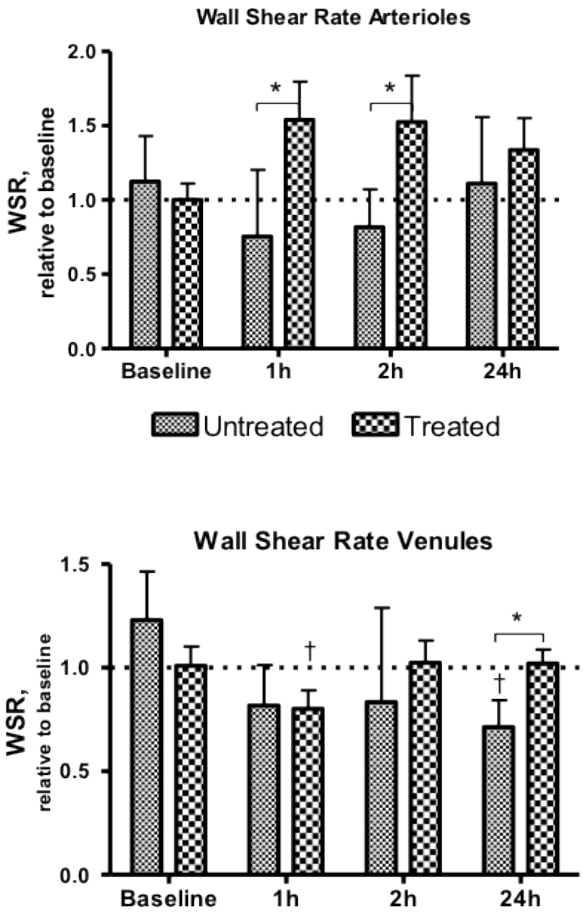

Figure 3.3. Wall shear rate data normalized relative to baseline for untreated and Np-treated groups. Values are shown as relative to baseline where 1.0 = 100% of baseline. Wall shear rate (s-1, mean ± SD) for each animal group were as follows: Untreated (arterioles [A]: 74.7 ± 26.7, n = 7; venules [V]: 45.3 ± 10.1, n = 6); Np-Treated [A]: 72.5 ± 30.1, n = 8; [V]: 53.8 ± 15.0, n = 6); with 'n' indicating number of vessels included.

3.5.5 Leukocyte Count

The graphs relating to rolling and immobilized leukocytes are presented in ***Figure 3.4***. The data is presented as fractions from the total amount of leukocytes counted in all time points. Rolling leukocytes, defined as those moving at a lower velocity than the vessel blood flow, were observed to remain constant for the entire experiment. Thus, no statistical significance could be found for this particular parameter. Immobilized leukocytes were reportedly more predominant in the *untreated* group, reaching more than 50% of all quantified sticking leukocytes for that group at the 2h mark. Nanoparticle treatment induced a significant reduction in leukocyte activation as seen by the immobilized fraction remaining at about 30% post-ischemia. At the 24h time point, immobilized leukocytes for the treated group was slightly greater than the untreated group though not found to be statistically significant.

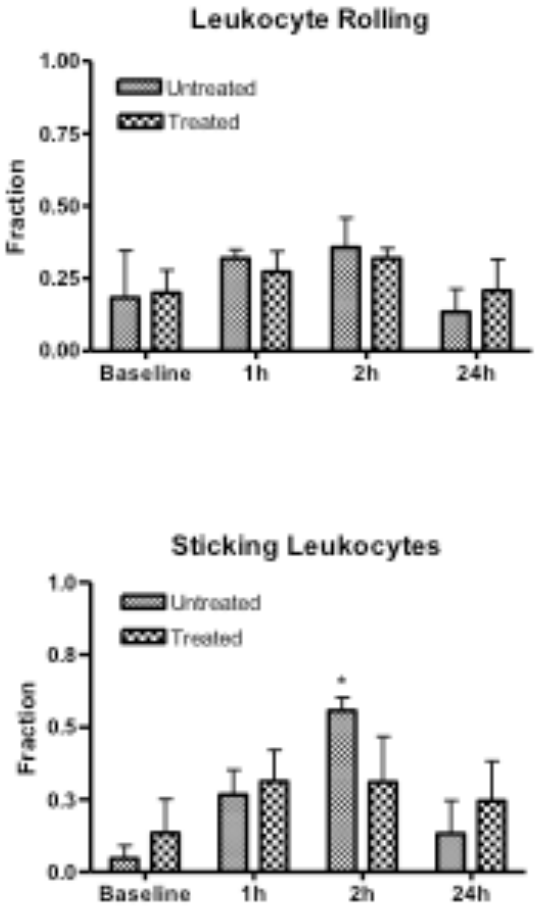

Figure 3.4. Leukocyte count for untreated and Np-treated groups.
Leukocyte data profile fraction. The values represent the fraction of leukocytes observed for that particular time point as compared to the total of leukocytes observed for all time points within the same individual. A value of 0.25 in the immobilized leukocyte graph represents that out of all the leukocytes measured as immobilized, one quarter of them were seen during that corresponding time point. Values are given as percentages ± SD. *P < 0.05 for comparison against *Untreated* group.

3.5.6 Tissue Survivability

The histological data is summarized on **Figure 3.5**. All immunohistochemistry measurements were performed on fixed tissue collected at 24 hours post-ischemia. Panel (A) breaks down cell death into early and late apoptotic and necrotic cell fates while panel (B) shows the absolute summation of these two distinct cell fates. Under

normal, baseline conditions, apoptosis and necrosis are observed at the same percentage and rate, namely close to 8%. The control group further demonstrated significantly lower amounts of death for both pathways. The injection of the nanoparticles caused a small reduction in cell death as compared to the untreated group, particularly apoptotic dependent. Yet, the two studied groups presented statistically equivalent tissue outcomes.

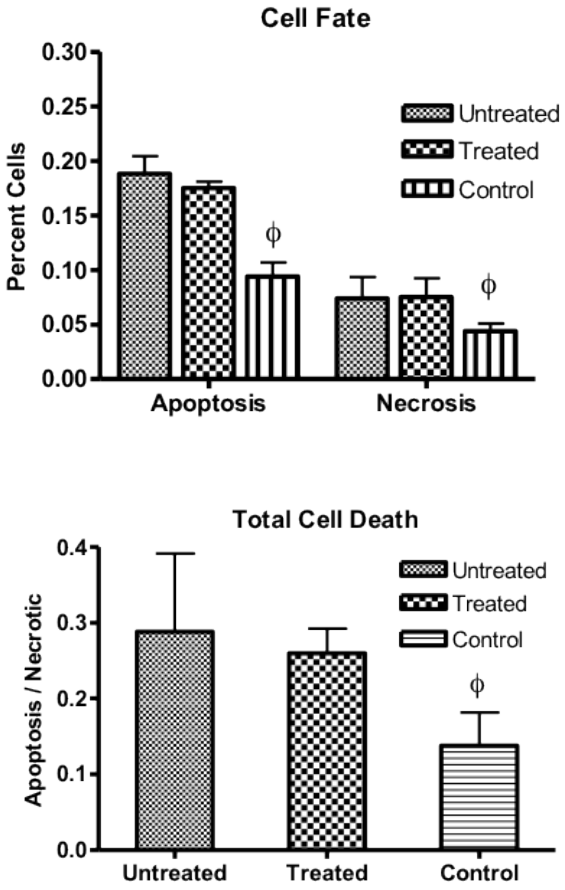

Figure 3.5. Histology data for untreated and Np-treated groups.
Cell fate count via immunohistochemistry on tissue collected at 24h post ischemia and fixed on formaldehyde. Panel A divides the data into apoptotic and necrotic cell fates. Panel B reports the summation of apoptotic and necrotic cells. ΦP > 0.05 when comparing against untreated and treated groups.

3.6 Discussion

The nanoparticles here proposed and used are ideal for situations of organ ischemia or even multi-organ ischemia injuries. Additionally, scenarios of major surgical procedures such as cardiac, thoracic, organ transplant and peripheral vascular surgery are optimal for the use of this therapeutic avenue. Given the fact that the nanoparticles can be localized and sustained in a specific, confined region of the body, this approach becomes truly ideal for the clinical situations aforementioned.

There have been reportedly downsides to Nitric Oxide delivery as a therapeutic intervention owing to the elevated levels of methemoglobin [1]. It is plausible that the excessive levels of NO within the circulation, or within a specified region, actually generate too high levels of methemoglobin, causing injury cascades to initiate that otherwise wouldn't for situations of systemic need such as hemorrhage shock or trauma. A reasonable solution would consist in reducing the dosage

From the capillary perfusion data, along with the hemodynamic parameters, it is possible to infer that perfusion rates were not altered significantly between the groups. Hence it is safe to conclude that perfusion itself was not an impactful or important parameter towards tissue outcome.

Even though the nanoparticle being used is supposed to deliver nitric oxide to the targeted tissue, vasodilation is not expected since the blood vessels are relaxed. This effect would be visible in situations where vasoconstriction would certainly occur, such as the cases for hemorrhagic shock or sepsis [9, 42]. The data does

confirm a higher degree of reperfusion for the treated group, putatively caused by the presence of the nanoparticles.

Furthermore, although there are no predicted shear rates for the activation of eNOS and its subsequent benefic effects, it is safe to assume that the sharp increase in shear forces in the vascular endothelium will cause an anti-inflammatory effect via eNOS activation.

The leukocyte quantification behaved as expected, where rolling leukocytes, even after corrections for flow, remain roughly unaltered throughout the protocol. Both groups presented rolling leukocytes at the same rate. However, the nanoparticle treated group demonstrated that during reperfusion, the level of inflammation and ultimate leukocyte activation is much more diminished, as seen by the halving of the measured fraction at the 2h time point. This is of particular importance as the NO delivering nanoparticles are supposed to deliver NO and cause a decline in inflammatory response. Thus, this is evidence that the sterile inflammation is being mitigated via the administration of this vehicle. A plausible reason as to why immobilized leukocytes were observed to be higher for the treated group 24h post ischemia might be due to the high presence of nanoparticles in a confined region of tissue where the nanoparticles themselves provoke the immune system to eliminate them. Previously, S-nitrosothiol types of nanoparticles have been found to form aggregates due to the cysteine bonds being formed after the NO payload is delivered [47].

Interestingly, the reduction in leukocytes had little or no bearing to tissue outcome, suggesting that perhaps their derived damage is not as prevalent or predominant for the scenarios here observed.

In spite of the differences aforementioned, tissue death outcome was not significantly averted with the proposed treatment and dosage. Aside from the mentioned high dosage concern, another factor plays an important role. That of the damage derived from ischemia itself. For the nanoparticle to have a noticeable effect, the reperfusion injury must be high. As such, the reperfusion injury caused in this study was kept at a minimum, enabling the nanoparticle intervention too narrow of a window to affect the outcome discernibly. There was simply not enough time for the buildup of superoxide and other metabolites that could cause further damage. Moreover, too much nitric oxide could react with superoxide to generate peroxynitrite, further damaging cell's membranes, lipids, etc, and hence contributing to the overall tissue damage.

As it can be seen, dosage and timing are crucial parameters to understand and delineate the therapeutic range and effect of interventions such as the nanoparticles here studied. In conclusion, the NO nanoparticles have potential though further research needs has to be done, particularly in pharmokinetics and overall safety.

IV. Concluding Remarks, Limitations and Future Directions

4.1 Conclusion

We have shown the development of a more reproducible and controllable device for the study of ischemia in the open window chamber model when compared against previous proposed models [1, 4, 6].

The damage secondary to ischemia is widely accepted in a huge variety of disease modes and pathological conditions but the reperfusion injury has not been properly emphasized or fully characterized. The reasons for such limited knowledge is partially due to the pragmatically more difficult techniques that must be employed and the consequentially more time-consuming research in identifying specific biochemical pathways or genes that might be at the core of a particular pathogenesis. But it is also because of the inherent limitations and problems of the ischemic models themselves where a lack of fine control is pervasive. In other words, the huge variability that one sees in physiological response is partially caused by the wide range in degrees of damage that one is eliciting to the tissue.

Very little research indeed has been done in comparing tourniquet and compressive ischemic models, with one particular study being done in the nineties [6]. In that particular study, however, the window chamber was divided in two and one side was subjected to tourniquet damage and the other to compressive injury. The experiment implies an enormous assumption where the two sides of the chamber have little or no influence on one another.

4.2 Limitations of the study

Inherent limitations lie within the fact that both forms of ischemic damage are not completely clinically translatable, considering there is a great deal of control over the damage. The controlled protocol allows for a more in-depth analysis where parameters can be assessed without confounding variables. In a realistic situation, the pressure that the tissue will experience will in fact be highly complex, both spatially and temporally.

In vivo studies of therapeutic interventions, such as nanoparticles, will always be subject to clinical validation involving real patients. Such limitations are inherent to every situation, arising from the higher complexity the human system presents.

Furthermore, comorbidities and aggravating factors that are not easily reproducible, quantifiable or even readily predictable may interfere with the ultimate outcome of any proposed therapeutic avenue. This study utilized only extremely healthy animals for the measurements, whereas in factual situations, patients might possess narrower cardiovascular and microcirculatory homeostatic capabilities. This is even more accentuated for vascular inflammatory diseases that are often underlined by cases of smoking, sedentariness, drug abuse, hypertension, hypercholesterolemia, stress, chronic inflammations, amongst others conditions.

Ultimately, clinical validation and extensive regulatory approval ought to be undertaken in order to fully substantiate the therapeutic effectiveness of any proposed intervention.

Another overarching limitation is that ischemia is still a very broad term to describe an intricate and highly complex process of different injuries affecting distinct tissues to varying extents. These clear variations can thus cause disparate results from one study to the next. Ischemia is a term applied to a great many injuries but they are not entirely equivalent and it is not always straightforward and simple to generalize findings from one scenario to another. There is therefore a potential promiscuity in terms of research.

The main limitation of the study is that although it deals with pressure-derived ischemia in an attempt to better elucidate and treat ischemic conditions that affect patients suffering from ulcers or bedsores, the injuries generated in this study are acute ones, rather than chronic. The aforementioned conditions are characterized by the localized chronic /reperfusion injury that eventually progress to the symptomatic known ischemia pathologies.

4.3 Future directions

The system and model thus presented is ideal for the study of ischemic-type injuries and all of its derivatives. The apparatus constructed enables the researcher to precisely control and fine tune the amount of pressure being imparted onto the tissue, providing superb reproducibility.

Additional biochemical validation is required for future research. To that extent, it is proposed that microvascular pO_2 experiments be performed via noninvasive phosphorescence quenching method (PQM) [56, 57]. This method is well

established and has been used previously, with the potential to give valuable insight into the mechanisms and efficacy of future proposed interventions to ischemia [9], including the one here expounded.

The model used empowers the researcher a myriad of possible experimental designs not only due to the superior control of the pressure being applied to the tissue but also to its spatial-temporal control. Choosing a specified pressure and applying the corresponding weight onto the apparatus for interleaving periods of time before or after a full ischemia can readily be designed for the study of pre or post-conditioning, respectively. It is conceivable that remote pre/post conditionings could also be studied.

Another entirely different experiment would be to drop a known mass from a certain height in order to study blunt trauma damage to the tissue. The known height and mass of the object yields a kinetic and potential energy that can be finely controlled.

The possibilities are virtually limitless once the user-related variables that caused non-reproducible effects from the previous model are circumvented.

Of notice is the possibility to more closely study the mesoscopic phenomena in the microcirculation by having increasingly smaller diameters for the tourniquet and comparing the microhemodynamic parameters between the groups. The question would be at what point does the mesoscopic scale truly holds. This is the central issue in the assumptions previously mentioned in past studies [6].

4.4 Nanoparticle delivery system and its potential

Additional studies could be envisioned to utilize No delivering nanoparticles towards the treatment or alleviation of typical inflammatory diseases that affect the cardiovascular system [58]. These include atherosclerosis, pulmonary infections, amongst others.

A more philosophical line of inquiry concerns the real intended role of ROS and RNS. That is to say, do these compounds simply cause DNA damage, cell death and injury and are generated unintentionally by the cells or do they perform a controlled and deliberate function of containing the spread of disease or infection within its host? Alternatively, these reactive species could have been initially generated simply because the cell has no other choice but to thermodynamically generate them and later on through evolution and adaptation, the organism gained the capacity to use them for damage control. This enquiry is a fundamental one because the approach to target ROS or RNS reduction is implicitly a stance or an answer to the question. At any rate, this question in particular is beyond the scope of this study and not easily answered since it requires one to assign judgments of value onto natural phenomena, a step that should never be taken lightly. Interestingly, one study done with pressure ulcers and ischemia demonstrated that the damage due to oxidation was not preventable in older animals, thus corroborating to the idea that oxidative shielding is indeed a mechanism of defense [55].

The question of whether every pathological condition is at heart an inflammatory condition is an interesting postulation and way of understanding disease

states. Virtually a wide range of conditions could be treated, or at the least mitigated, by the use of anti-inflammatory compounds. Inflammatory bowel disease, Chron's disease, colitis, and a certain number of autoimmune disorders are examples of possibilities yet to be tackled by the medical community.

Autophagy seems like an interesting avenue of research due to the debate surrounding it. There is no established consensus over whether it is a necessary adaptive response or an exaggerated response from the cells but recent studies have been hinting at autophagy possessing protective roles [36].

Concerning the innate immune system, there is currently no consensus over the functional role of leukocytes being recruited to ischemic tissue due to sterile inflammation [59]. It is possible that they further contribute to collateral damage of the tissue or indeed provide a means towards the resolution of the insult. This is a central question that ought to be answered in the near future as the two alternatives demand diametrically opposed modes of therapies.

Appendix:

A.1 Supplemental Figures

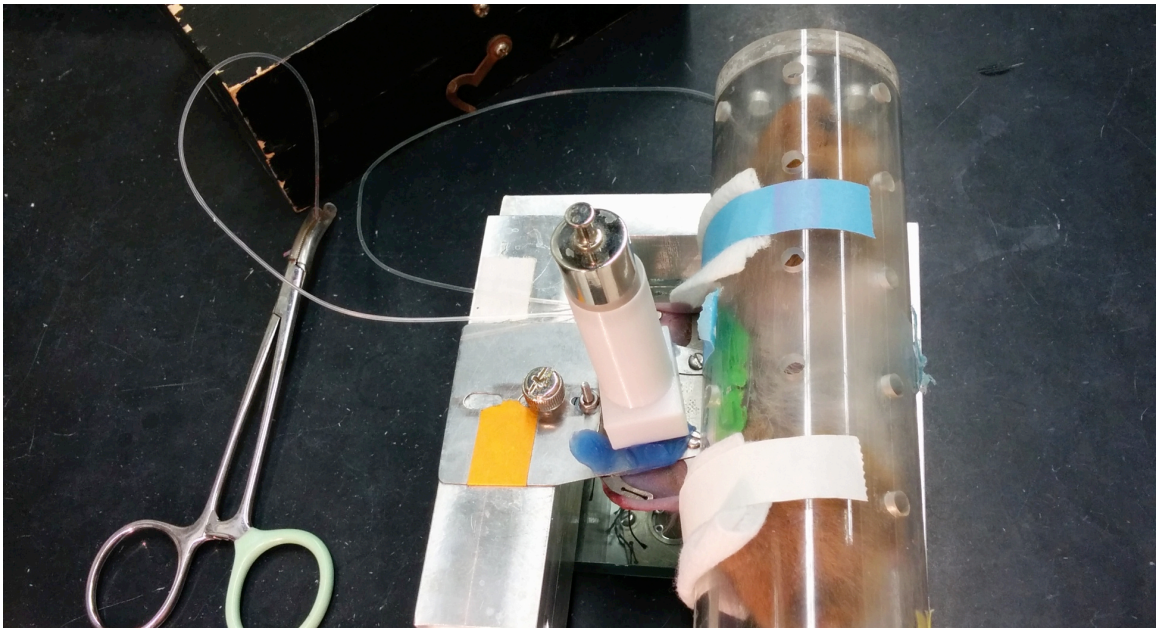

Figure 1.1. Photograph of the apparatus mounted in a live hamster for ischemia insult.

References

[1] H.K. Eltzschig, T. Eckle, Ischemia and reperfusion--from mechanism to translation, Nature medicine, 17 (2011) 1391-1401.

[2] R.J. Schauer, A.L. Gerbes, D. Vonier, H. Meissner, P. Michl, R. Leiderer, F.W. Schildberg, K. Messmer, M. Bilzer, Glutathione protects the rat liver against reperfusion injury after prolonged warm ischemia, Annals of surgery, 239 (2004) 220-231.

[3] F. Di Lisa, P. Bernardi, Mitochondria and ischemia-reperfusion injury of the heart: fixing a hole, Cardiovasc Res, 70 (2006) 191-199.

[4] M.D. Menger, M.W. Laschke, B. Vollmar, Viewing the microcirculation through the window: Some twenty years experience with the hamster dorsal skinfold chamber, European Surgical Research, 34 (2002) 83-91.

[5] D. Nolte, H. Zeintl, M. Steinbauer, S. Pickelmann, K. Messmer, Functional capillary density: an indicator of tissue perfusion?, Int J Microcirc Clin Exp, 15 (1995) 244-249.

[6] D. Nolte, M.D. Menger, K. Messmer, Microcirculatory models of ischaemia-reperfusion in skin and striated muscle, Int J Microcirc Clin Exp, 15 Suppl 1 (1995) 9-16.

[7] B. Endrich, K. Asaishi, A. Gotz, K. Messmer, Technical report--a new chamber technique for microvascular studies in unanesthetized hamsters, Res Exp Med (Berl), 177 (1980) 125-134.

[8] S. Hak, N.K. Reitan, O. Haraldseth, C. de Lange Davies, Intravital microscopy in window chambers: a unique tool to study tumor angiogenesis and delivery of nanoparticles, Angiogenesis, 13 (2010) 113-130.

[9] D. Ortiz, M. Barros, S. Yan, P. Cabrales, Resuscitation from hemorrhagic shock using polymerized hemoglobin compared to blood, The American journal of emergency medicine, 32 (2014) 248-255.

[10] P. Cabrales, F. Meng, S.A. Acharya, Tissue oxidative metabolism after extreme hemodilution with PEG-conjugated hemoglobin, Journal of applied physiology, 109 (2010) 1852-1859.

[11] J.M. Devoisselle, S. Begu, C. Tourne-Peteilh, T. Desmettre, S. Mordon, In vivo behaviour of long-circulating liposomes in blood vessels in hamster inflammation and septic shock models-use of intravital fluorescence microscopy, Luminescence : the journal of biological and chemical luminescence, 16 (2001) 73-78.

[12] G.M. Palmer, A.N. Fontanella, S. Shan, G. Hanna, G. Zhang, C.L. Fraser, M.W. Dewhirst, In vivo optical molecular imaging and analysis in mice using dorsal window chamber models applied to hypoxia, vasculature and fluorescent reporters, Nature protocols, 6 (2011) 1355-1366.

[13] Lyudmila Sikora, Savita P. Rao , P. Sriramarao, Selectin-dependent rolling and adhesion of leukocytes in nicotine-exposed microvessels of lung allografts, American Journal of Physiology-Lung Cellular and Molecular Physiology, 285 (2003) L654–L663.

[14] M.W. Laschke, B. Vollmar, M.D. Menger, The Dorsal Skinfold Chamber: Window into the Dynamic Interaction of Biomaterials with Their Surrounding Host Tissue, European Cells & Materials, 22 (2011) 147-167.

[15] W. Jia, N. Tran, V. Sun, M. Marincek, B. Majaron, B. Choi, J.S. Nelson, Photocoagulation of dermal blood vessels with multiple laser pulses in an in vivo microvascular model, Lasers in surgery and medicine, 44 (2012) 144-151.

[16] Z. Bajory, A. Szabo, I. Kiraly, L. Pajor, K. Messmer, Involvement of nitric oxide in microcirculatory reactions after ischemia-reperfusion of the rat urinary bladder, European surgical research. Europaische chirurgische Forschung. Recherches chirurgicales europeennes, 42 (2009) 28-34.

[17] E. Crimi, L.J. Ignarro, C. Napoli, Microcirculation and oxidative stress, Free radical research, 41 (2007) 1364-1375.

[18] H.H. Lu, Y.M. Wu, W.T. Chang, T. Luo, Y.C. Yang, H.D. Juo, I. Liau, Molecular imaging of ischemia and reperfusion in vivo with mitochondrial autofluorescence, Analytical chemistry, (2014).

[19] X. Guo, H. Sesaki, X. Qi, Drp1 stabilizes p53 on the mitochondria to trigger necrosis under oxidative stress conditions, in vitro and in vivo, The Biochemical journal, (2014).

[20] V.V. Shuvaev, J. Han, S. Tliba, E. Arguiri, M. Christofidou-Solomidou, S.H. Ramirez, H. Dykstra, Y. Persidsky, D.N. Atochin, P.L. Huang, V.R. Muzykantov, Anti-

inflammatory effect of targeted delivery of SOD to endothelium: mechanism, synergism with NO donors and protective effects in vitro and in vivo, PloS one, 8 (2013) e77002.

[21] U. Forstermann, T. Munzel, Endothelial nitric oxide synthase in vascular disease: from marvel to menace, Circulation, 113 (2006) 1708-1714.

[22] Z. Hu, Y. Xiong, X. Han, C. Geng, B. Jiang, Y. Huo, J. Luo, Acute mechanical stretch promotes eNOS activation in venous endothelial cells mainly via PKA and Akt pathways, PloS one, 8 (2013) e71359.

[23] D.E. Ingber, Tensegrity: the architectural basis of cellular mechanotransduction, Annu Rev Physiol, 59 (1997) 575-599.

[24] Ingrid Fleming, R. Busse, Signal Transduction of eNOS activation, Cardiovascular Research, (1999) 532-541.

[25] M.L. Circu, T.Y. Aw, Glutathione and modulation of cell apoptosis, Biochimica et biophysica acta, 1823 (2012) 1767-1777.

[26] H.-J. Hsieh, C.-A. Liu, B. Huang, A.H. Tseng, D.L. Wang, Shear-induced endothelial mechanotransduction: the interplay between reactive oxygen species (ROS) and nitric oxide (NO) and the pathophysiological implications, Journal of Biomedical Science, 21 (2014).

[27] D.E. Conway, M.T. Breckenridge, E. Hinde, E. Gratton, C.S. Chen, M.A. Schwartz, Fluid shear stress on endothelial cells modulates mechanical tension across VE-cadherin and PECAM-1, Current biology : CB, 23 (2013) 1024-1030.

[28] S. Momi, F. Impagnatiello, M. Guzzetta, R. Caracchini, G. Guglielmini, R. Olivieri, A. Monopoli, P. Gresele, NCX 6560, a nitric oxide-releasing derivative of atorvastatin, inhibits cholesterol biosynthesis and shows anti-inflammatory and anti-thrombotic properties, European journal of pharmacology, 570 (2007) 115-124.

[29] A. Dejam, C.J. Hunter, A.N. Schechter, M.T. Gladwin, Emerging role of nitrite in human biology, Blood cells, molecules & diseases, 32 (2004) 423-429.

[30] F.B. Jensen, The role of nitrite in nitric oxide homeostasis: a comparative perspective, Biochimica et biophysica acta, 1787 (2009) 841-848.

[31] I. Azarov, K.T. Huang, S. Basu, M.T. Gladwin, N. Hogg, D.B. Kim-Shapiro, Nitric oxide scavenging by red blood cells as a function of hematocrit and oxygenation, The Journal of biological chemistry, 280 (2005) 39024-39032.

[32] G.W. Schmid-Schonbein, The damaging potential of leukocyte activation in the microcirculation, Angiology, 44 (1993) 45-56.

[33] T. Gobbetti, N. Cenac, J.P. Motta, C. Rolland, L. Martin, P. Andrade-Gordon, M. Steinhoff, E. Barocelli, N. Vergnolle, Serine protease inhibition reduces post-ischemic granulocyte recruitment in mouse intestine, The American journal of pathology, 180 (2012) 141-152.

[34] J.F.M. VIVEK KOHLI, REX C. BENTLEY, and PIERRE–ALAIN CLAVIEN, Calpain Mediates Ischemic Injury of the Liver Through Modulation of Apoptosis and Necrosis, Gastroenterology, 116 (1999).

[35] S. Carloni, M.C. Albertini, L. Galluzzi, G. Buonocore, F. Proietti, W. Balduini, Increased autophagy reduces endoplasmic reticulum stress after neonatal hypoxia-ischemia: role of protein synthesis and autophagic pathways, Experimental neurology, 255 (2014) 103-112.

[36] X. Zhang, H. Yan, Y. Yuan, J. Gao, Z. Shen, Y. Cheng, Y. Shen, R.R. Wang, X. Wang, W.W. Hu, G. Wang, Z. Chen, Cerebral ischemia-reperfusion-induced autophagy protects against neuronal injury by mitochondrial clearance, Autophagy, 9 (2013) 1321-1333.

[37] S. Miyata, G. Takemura, Y. Kawase, Y. Li, H. Okada, R. Maruyama, H. Ushikoshi, M. Esaki, H. Kanamori, L. Li, Y. Misao, A. Tezuka, T. Toyo-Oka, S. Minatoguchi, T. Fujiwara, H. Fujiwara, Autophagic cardiomyocyte death in cardiomyopathic hamsters and its prevention by granulocyte colony-stimulating factor, The American journal of pathology, 168 (2006) 386-397.

[38] A.G. Thrift, D.A. Cadilhac, T. Thayabaranathan, G. Howard, V.J. Howard, P.M. Rothwell, G.A. Donnan, Global stroke statistics, International journal of stroke : official journal of the International Stroke Society, 9 (2014) 6-18.

[39] T. Mustoe, Understanding chronic wounds: a unifying hypothesis on their pathogenesis and implications for therapy, The American Journal of Surgery, 187 (2004) S65-S70.

[40] T. Jayakumar, C.C. Chang, S.L. Lin, Y.K. Huang, C.M. Hu, A.R. Elizebeth, S.C. Lin, C.S. Choy, Brazilin Ameliorates High Glucose-Induced Vascular Inflammation via Inhibiting ROS and CAMs Production in Human Umbilical Vein Endothelial Cells, BioMed research international, 2014 (2014) 403703.

[41] M.-L. Lazo-de-la-Vega-Monroy, C. Fernndez-Mej, Oxidative Stress in Diabetes Mellitus and the Role Of Vitamins with Antioxidant Actions, (2013).

[42] R. Lima, N.R. Villela, E. Bouskela, Microcirculatory effects of selective receptor blockade during hemorrhagic shock treatment with vasopressin: experimental study in the hamster dorsal chamber, Shock, 38 (2012) 493-498.

[43] D. Ortiz, J.C. Briceno, P. Cabrales, Microhemodynamic parameters quantification from intravital microscopy videos, Physiological measurement, 35 (2014) 351-367.

[44] A.G. Khandoga, A. Khandoga, C.A. Reichel, P. Bihari, M. Rehberg, F. Krombach, In vivo imaging and quantitative analysis of leukocyte directional migration and polarization in inflamed tissue, PloS one, 4 (2009) e4693.

[45] P. Cabrales, Examining and mitigating acellular hemoglobin vasoactivity, Antioxidants & redox signaling, 18 (2013) 2329-2341.

[46] B.Y. Owusu, R. Stapley, R.P. Patel, Nitric Oxide formation versus scavenging: The Red Blood Cell balancing act., Journal of Physiology, (2014).

[47] P. Nacharaju, C. Tuckman-Vernon, K.E. Maier, J. Chouake, A. Friedman, P. Cabrales, J.M. Friedman, A nanoparticle delivery vehicle for S-nitroso-N-acetyl cysteine: sustained vascular response, Nitric Oxide, 27 (2012) 150-160.

[48] G. Preissler, F. Lohe, U. Ebersberger, I. Huff, I. Bittmann, K. Messmer, K.W. Jauch, M.K. Angele, Recipient treatment with L-arginine attenuates donor lung injury associated with hemorrhagic shock, Transplantation, 87 (2009) 1602-1608.

[49] S.B. Cau, F.S. Carneiro, R.C. Tostes, Differential modulation of nitric oxide synthases in aging: therapeutic opportunities, Frontiers in physiology, 3 (2012) 218.

[50] M.D. Howard, E.D. Hood, B. Zern, V.V. Shuvaev, T. Grosser, V.R. Muzykantov, Nanocarriers for vascular delivery of anti-inflammatory agents, Annual review of pharmacology and toxicology, 54 (2014) 205-226.

[51] Z. Cheng, A. Al Zaki, J.Z. Hui, V.R. Muzykantov, A. Tsourkas, Multifunctional nanoparticles: cost versus benefit of adding targeting and imaging capabilities, Science, 338 (2012) 903-910.

[52] C. Liong, D. Ortiz, E. Ao-Ieong, M.S. Navati, J.M. Friedman, P. Cabrales, Localized increase of tissue oxygen tension by magnetic targeted drug delivery, Nanotechnology, 25 (2014) 265102.

[53] M.J. Ernsting, M. Murakami, A. Roy, S.D. Li, Factors controlling the pharmacokinetics, biodistribution and intratumoral penetration of nanoparticles, J Control Release, 172 (2013) 782-794.

[54] D. Sorriento, A.V. Pascale, R. Finelli, A.L. Carillo, R. Annunziata, B. Trimarco, G. Iaccarino, Targeting Mitochondria as Therapeutic Strategy for Metabolic Disorders, TheScientificWorldJournal, 2014 (2014) 604685.

[55] J.M. Olivera Stojadinovic, Andrew Sawaya, Jonathan W. Bourne, Peter Torzilli, Juan Pablo de Rivero Vaccari, W. Dalton Dietrich, Robert W. Keane, Marjana Tomic-Canic, Deep Tissue Injury in Development of Pressure Ulcers: A Decrease of Inflammasome Activation and Changes in Human Skin Morphology in Response to Aging and Mechanical Load, PloS one, 8 (2013).

[56] A.G. Tsai, B. Friesenecker, M.C. Mazzoni, H. Kerger, D.G. Buerk, P.C. Johnson, M. Intaglietta, Microvascular and tissue oxygen gradients in the rat mesentery, Proceedings of the National Academy of Sciences of the United States of America, 95 (1998) 6590-6595.

[57] H. Kerger, pO2 measurements by phosphorescence quenching: characteristics and applications of an automated system, Microvascular Research, 65 (2003) 32-38.

[58] F. Calabrese, Infection and inflammation in the cardiovascular system, Cardiovascular Research, 60 (2003) 1-4.

[59] G. Courties, M.A. Moskowitz, M. Nahrendorf, The innate immune system after ischemic injury: lessons to be learned from the heart and brain, JAMA neurology, 71 (2014) 233-236.